



HAL
open science

Combining T/P altimetric data with hydrographic data to estimate the mean dynamic topography of the North Atlantic and improve the geoid

P. Legrand, H. Mercier, T. Reynaud

► To cite this version:

P. Legrand, H. Mercier, T. Reynaud. Combining T/P altimetric data with hydrographic data to estimate the mean dynamic topography of the North Atlantic and improve the geoid. *Annales Geophysicae*, 1998, 16 (5), pp.638-650. hal-00329083

HAL Id: hal-00329083

<https://hal.science/hal-00329083>

Submitted on 18 Jun 2008

HAL is a multi-disciplinary open access archive for the deposit and dissemination of scientific research documents, whether they are published or not. The documents may come from teaching and research institutions in France or abroad, or from public or private research centers.

L'archive ouverte pluridisciplinaire **HAL**, est destinée au dépôt et à la diffusion de documents scientifiques de niveau recherche, publiés ou non, émanant des établissements d'enseignement et de recherche français ou étrangers, des laboratoires publics ou privés.

Combining T/P altimetric data with hydrographic data to estimate the mean dynamic topography of the North Atlantic and improve the geoid

P. LeGrand¹, H. Mercier¹, and T. Reynaud^{1,2}

¹ Laboratoire de Physique des Océans, Unité mixte CNRS-IFREMER-Université de Bretagne Occidentale, IFREMER centre de Brest, B.P. 70, F-29280 Plouzané, France

² Now at LEG1/MEOM, Institut de Mécanique de Grenoble, B.P. 53, F-38041 Grenoble CEDEX, France

Received: 4 July 1997 / Revised: 9 January 1998 / Accepted: 16 January 1998

Abstract. The mean dynamic topography of the surface of the North Atlantic is estimated using an inverse model of the ocean circulation constrained by hydrographic and altimetric observations. In the North Atlantic, altimetric observations have no significant impact on the topography estimate because of the limited precision of available geoid height models. They have a significant impact, however, when uncertainties in the density field are increased to simulate interpolation errors in regions where hydrographic data are scarce. This result, which moderates the conclusion drawn by Ganachaud and co-workers of no significant contribution of altimetric observations to the determination of the large-scale steady circulation, reflects the simple idea that altimetric data are most useful near the surface of the ocean and in areas where the hydrography is poorly determined. One application of the present inverse estimate of the mean dynamic topography is to compute a geoid height correction over the North Atlantic which reduces the uncertainty in the geoid height expanded to spherical harmonic 40 down to a level of about 5 cm.

Key words. Oceanography: general (climate and interannual variability) · Oceanography: physical (general circulation; remote sensing)

1 Introduction

During the past few years, much has been learned on the variable component of the ocean circulation using the Topex/Poseidon (T/P) observations. The determination of the mean component of the circulation from altimetric measurements, however, is still hampered by

the lack of a precise estimate of the geoid height. The geoid height is the elevation the surface of the ocean would have if it were at rest, and it must be subtracted from the altimetric sea surface height to determine the dynamic topography associated with oceanic currents. The error in existing geoid height models exceeds the dynamic topography signal for spherical harmonic degrees larger than 15 (Nerem *et al.*, 1994), and the ability of altimetric data to determine the mean circulation at spatial scales smaller than about 1000 km is therefore limited. Moreover, Ganachaud *et al.* (1997) find that the ability of altimetric observations to improve significantly the large-scale circulation derived from an inversion of hydrographic data is also limited, despite the fact that the geoid height error is smaller than the topographic signal at larger scales.

The impact of altimetric observations on the determination of the mean circulation is re-examined in this work using a finite difference inverse model (Mercier *et al.*, 1993) instead of the box inverse model used by Ganachaud *et al.* (1997). The finite difference model adjusts the density field, uses altimetric observations away from the location of hydrographic sections, and produces an estimate of the mean dynamic topography of the surface of the ocean over a regular grid (Le Traon and Mercier, 1992). The altimetric observations introduced in the model consist of an estimate of the mean dynamic topography obtained by subtracting the JGM-2 geoid height model from the mean sea surface height observed by T/P. The impact of these observations is evaluated by comparing the mean dynamic topography estimated by the model when the altimetric constraint is included to that estimated using in situ observational constraints only. Two outcomes are possible: (1) if the altimetric constraint is more precise, or as precise as the topography estimated by the inverse model using in situ observations only, then this constraint will have a significant impact and will improve the inverse solution; and (2) if the altimetric constraint is far less precise, it will have no significant impact on the inverse solution other than insuring that the solution is consistent with the

geodesic information contained in this constraint. In this case, the geoid height model obtained by subtracting the inverse topography estimate from the observed mean sea surface height (Roemmich and Wunsch, 1982) is likely to be more precise than existing geoid height models.

The study is divided into six sections. Following this introduction, Sect. 2 describes the direct altimetric estimate of the mean dynamic topography over the North Atlantic that will be used to constrain the inverse model. Section 3 describes a hydrographic estimate of the mean dynamic topography that illustrates the potential of in situ observations to determine the topography of the ocean. Section 4 presents an inverse estimate of the mean dynamic topography calculated by a combination of dynamical constraints and hydrographic data and another estimate in which altimetric data are also incorporated. In accordance with Ganachaud *et al.*'s (1997) conclusion, altimetric observations are found to be fully consistent with geostrophic dynamics and hydrographic observations, but to weakly constrain the mean dynamic topography estimate in the North Atlantic. Section 5, however, shows that altimetric data do constrain this estimate if the density field is poorly known, and can provide useful information in regions like the Southern Ocean that are poorly sampled by the hydrographic data base. The impact of uncertainties in the density field and the differences between the present calculation and that of Ganachaud *et al.* (1997) are discussed in this section. Finally, Sect. 6 summarizes the results of this study and concludes by using the inverse model's topography estimate to calculate a geoid height correction in the North Atlantic. The precision of the corrected geoid height is on the order of 5 cm at spatial scales of about 500 km.

2 An altimetric estimate using T/P data and the JGM-2 geoid

One way to estimate the mean dynamic topography of the surface of the ocean is to subtract an estimate of the geoid height from the mean sea surface height observed by an altimeter. This altimetric estimate will serve as a useful basis of comparison for other estimates and will be used to constrain the inverse calculations of Sects. 4 and 5. In this section, the geoid height computed using the JGM-2 gravimetry field solution (Tapley *et al.*, 1994) is subtracted from the mean of 2 y of T/P sea surface height observations (cycles 2 to 75). Corrections are applied to the T/P sea surface height measurements to remove the influence of the troposphere (dry and wet), of oceanic waves, and of the inverse barometer effect. The difference between the sea surface height and the geoid height yields an estimate of the mean dynamic topography along satellite tracks in the North Atlantic between 20°N and 50°N. This estimate is averaged onto a 5° longitude by 4° latitude grid (Fig. 1) to take advantage of the higher precision of the geoid model at larger scales, while approximately preserving the main features of the Gulf Stream and of the subtropical gyre (Fig. 2).

The JGM-2 geoid height uncertainty (Tapley *et al.*, 1994) is much larger than the uncertainty in the mean sea surface height observed by T/P and is the main source of uncertainty in the altimetric estimate of the mean dynamic topography. The uncertainty in the geoid height estimate is calculated using a spatial autocorrelation function (Rapp, Le Traon, personal communication, 1994) corresponding to an expansion of the geoid to spherical harmonic 40. The error covariance of the geoid height is divided by 2 prior to the mean dynamic

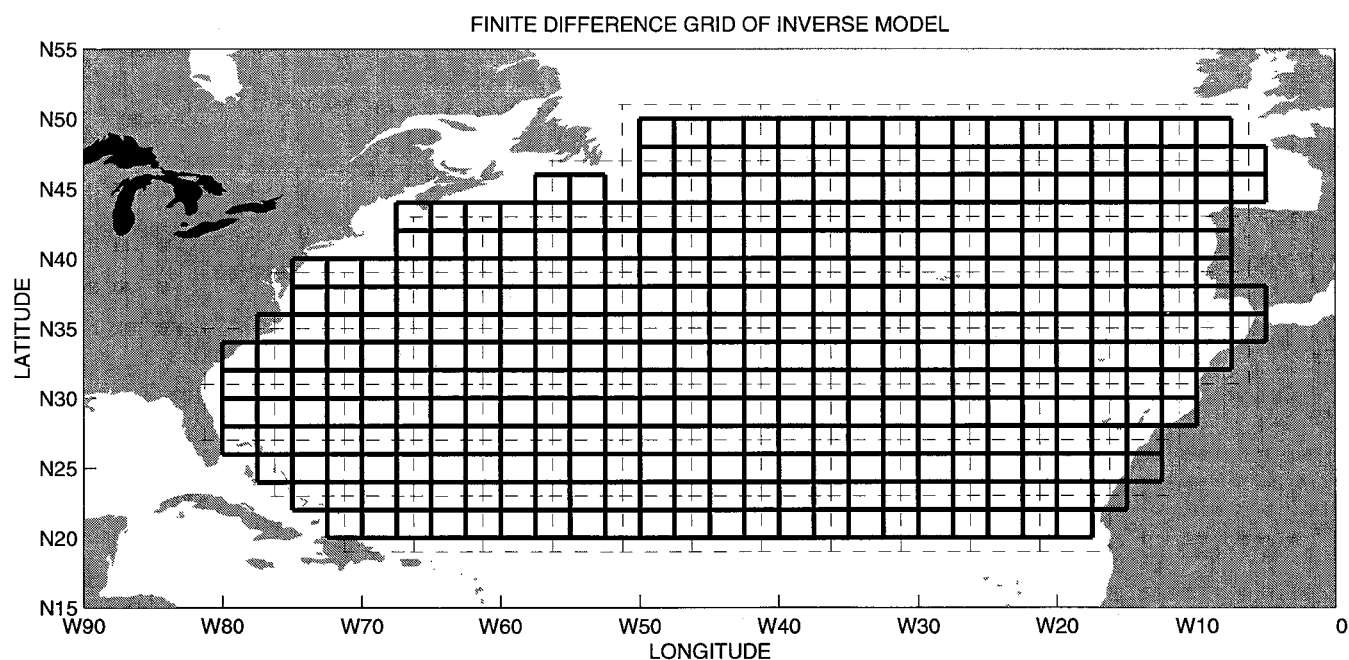


Fig. 1. The *solid lines* represent the 2.5° longitude \times 2° latitude density grid of the inverse model. The *thin dashed lines* represent the 5° longitude \times 4° latitude grid used to compute the altimetric estimate of mean dynamic topography (Sect. 2)

MEAN DYNAMIC TOPOGRAPHY CALCULATED USING T/P SSH AND JGM2

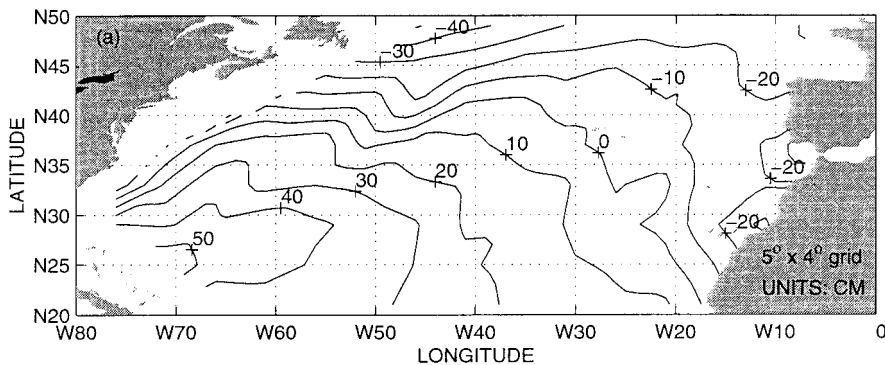


Fig. 2. Mean dynamic topography calculated on the 5° longitude \times 4° latitude grid using T/P observations of the mean sea surface height and the JGM-2 geoid height

topography uncertainty calculation to take into account that the geoid height error is smaller over oceans than over land (Rapp, Le Traon, personal communication, 1994), and the resulting geoid height uncertainty is about 18 cm. The uncertainty in the mean sea surface height is estimated in the $5^\circ \times 4^\circ$ boxes using the T/P observations. The number of independent observations inside a box is determined assuming that the oceanic mesoscale variability, which is the main source of uncertainty in the mean sea surface height, has a decorrelation scale of 100 km. The resulting sea surface height uncertainty is less than 5 cm in the interior of the ocean and is about four times smaller than the geoid height uncertainty. The uncertainty in the mean dynamic topography calculated using the T/P sea surface height and the JGM-2 geoid is roughly uniform over the 20°N – 50°N domain and is on the order of 20 cm. This uncertainty corresponds to an uncertainty in surface velocities averaged over 200 km on the order of 10 cm/s.

3 A diagnostic estimate using hydrographic data

The mean dynamic topography of the North Atlantic is diagnosed from a compilation of more than 100 000 hydrographic stations collected over the past 70 years. About 25 000 of these stations are deeper than 1000 m

(Fig. 3). Some recent data come from the Laboratoire de Physique des Océans compilation, but most data come from the large historic data set of the US National Oceanographic Data Center. The station density profiles are gridded onto the inverse model 2.5° longitude \times 2° latitude finite difference grid (Fig. 1). Their variance gives an estimate of the uncertainty in the gridded density field (see the Appendix).

The thermal wind equation is integrated assuming a reference level of no motion at 3000 decibars or the bottom, which ever is shallower, up to the surface to calculate surface velocities. These velocities are integrated with respect to horizontal coordinates to estimate, using the geostrophic balance, the mean dynamic topography over the North Atlantic. The arbitrary integration constant is determined by the condition that the volume of the North Atlantic is fixed in a steady state calculation. This condition sets the spatial mean of the dynamic topography over the basin, this spatial mean being determined by the T/P altimetric observations for consistency with the altimetric topography estimate of the previous section.

The mean dynamic topography diagnosed from hydrographic data is consistent with what is known of the ocean circulation. The mean Gulf Stream is apparent as a front a few degrees wide as well as the North Atlantic extension (Fig. 4a). Recirculation zones are

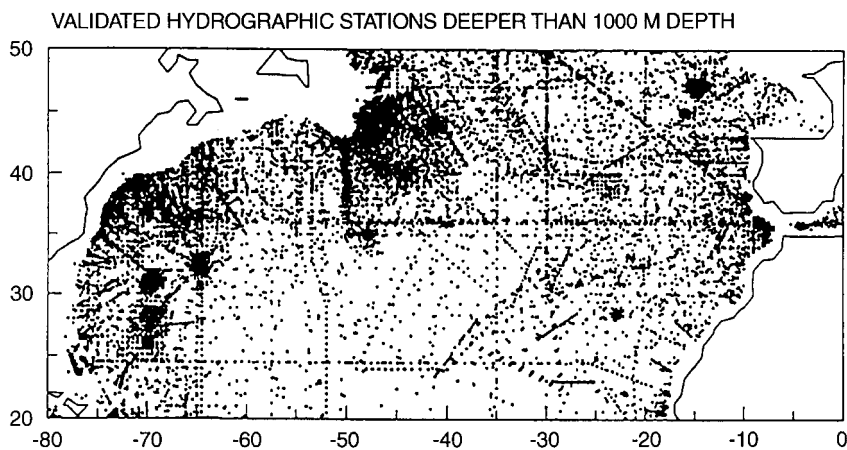


Fig. 3. Distribution, after quality control, of the hydrographic stations in the data compilation that are deeper than 1000 m depth

MEAN DYNAMIC TOPOGRAPHY DIAGNOSED FROM THE DENSITY FIELD

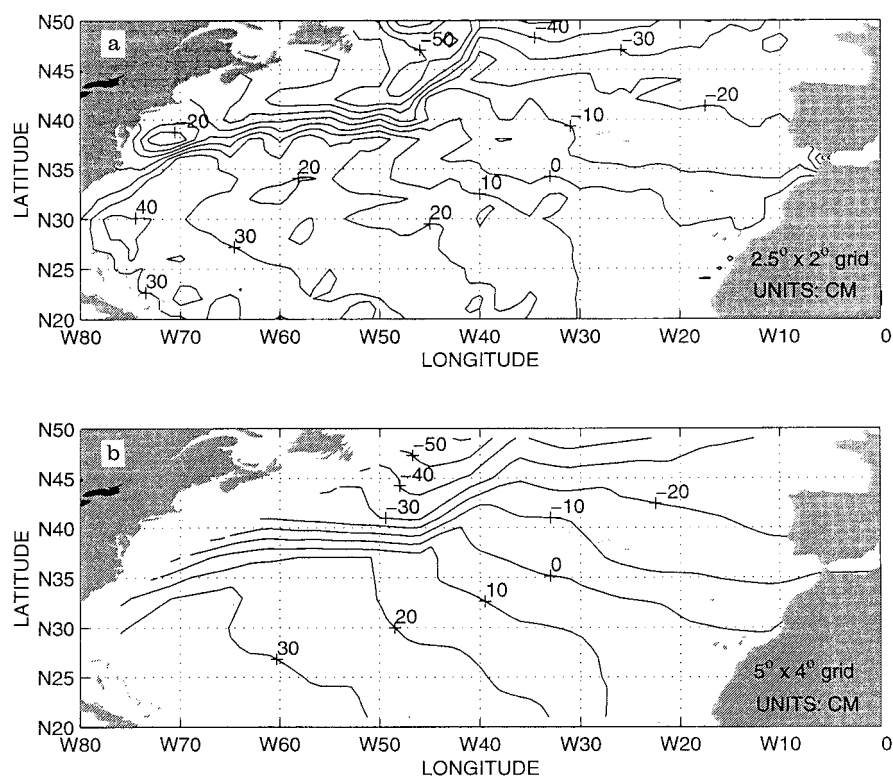


Fig. 4. **a** Mean dynamic topography (cm) diagnosed from the density field on the 2.5° longitude \times 2° latitude grid. **b** Same as **a** but averaged onto the 5° longitude \times 4° latitude grid

present north and south of the Gulf Stream (Fig. 4a). This estimate of the mean dynamic topography is averaged (Fig. 4b) on to the $5^\circ \times 4^\circ$ grid for comparison with the altimetric estimate (Fig. 2). In the hydrographic estimate (Fig. 4b), the isocontours which correspond to the Gulf Stream are almost zonal near Cape Hatteras and seem to reflect the separation of the Gulf Stream, whereas this separation is not apparent in the altimetric estimate (Fig. 2). The absence of Gulf Stream separation in the altimetric estimate may be caused by errors in the marine geoid height estimate. Thus, the mean dynamic topography diagnosed from the density field appears to be more consistent with what is known of the ocean circulation than the mean dynamic topography estimated from T/P data and the JGM-2 geoid.

The uncertainty in the hydrographic estimate of the mean dynamic topography is diagnosed from the uncertainty in the density field and the uncertainty in the reference velocities. The reference velocities are the velocities at the reference level of no motion and are assumed to be zero within reasonable uncertainties of 2 cm/s in the interior of the ocean, and 10 cm/s near the western boundary. These uncertainties contribute to less than 25% of the total topography uncertainty. The uncertainty in the topography averaged onto the $5^\circ \times 4^\circ$ grid is less than 10 cm everywhere except near the western boundary (Fig. 5). The uncertainty is also larger than 10 cm around $[30^\circ\text{W}, 20^\circ\text{N}]$, (Fig. 5) because of interpolation errors. Indeed, there are several bins in this area that do not contain enough stations to compute the mean density and its standard deviation, and these

quantities must be interpolated (Appendix). The spatial distribution of the topography uncertainty (Fig. 5) makes physical sense. It is maximum near the western boundary, where the uncertainty in the mean density field is largest because of the strong mesoscale variability. Except for the small region around $[30^\circ\text{W}, 20^\circ\text{N}]$, mentioned already, it is minimum in the relatively quiescent southeastern corner of the model domain. The uncertainty in the mean dynamic topography, diagnosed from the density field, is consistent, both in distribution and amplitude, with the temporal variability in the dynamic height directly estimated from T/P observations averaged onto a 5° longitude \times 2° latitude grid (White and Tai, 1995). This consistency indicates that the uncertainty in the mean dynamic topography, diagnosed from the density field, is mostly due to the oceanic variability. Globally, this uncertainty is smaller by a factor of 2 than the 20 cm uncertainty in the altimetric estimate of dynamic topography of section II. The mean dynamic topography estimated from hydrographic data is thus more precise than the one estimated from T/P and JGM-2.

4 Inverse estimates combining T/P altimetric data with hydrographic data

In this section, the mean dynamic topography of the North Atlantic is estimated using the inverse model of Mercier *et al.* (1993). The model finds an ocean circulation, and the associated dynamic topography,

UNCERTAINTY IN MEAN DYNAMIC TOPOGRAPHY DIAGNOSED FROM THE DENSITY FIELD

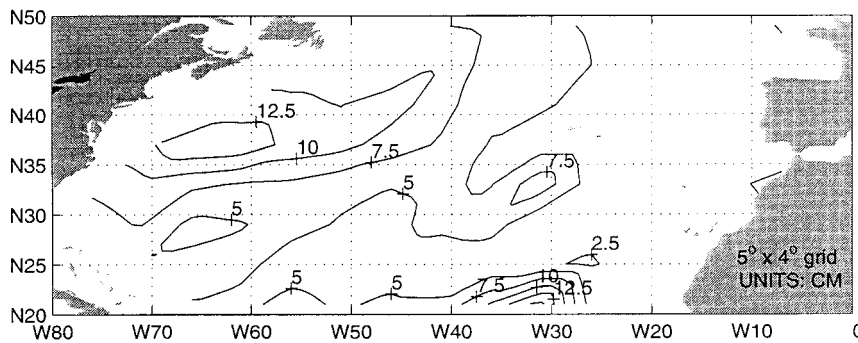


Fig. 5. Uncertainty (cm) in the $5^\circ \times 4^\circ$ mean dynamic topography estimate of Fig. 4b

that best fits in a least-square sense the hydrographic and altimetric observational constraints with simplified dynamical constraints relevant to the large-scale ocean circulation. The observations and the dynamics are discretized onto a 2.5° longitude by 2° latitude grid (Fig. 1). Thus, the model provides an estimate of the mean dynamic topography with a spatial resolution on the order of 200 km. The inverse model provides a realistic calculation of the uncertainty in the mean dynamic topography because it accounts for uncertainties in the mean density field. A similar inverse calculation of the mean dynamic topography was done by Le Traon and Mercier (1992). The present calculation is improved compared to their calculation in a number of points: (1) altimetric observations are included in the model; (2) the density field is estimated from a large historic data set instead of a limited hydrographic data base; and (3) the uncertainty in the density field is directly estimated from the hydrographic data and is more realistic (see the Appendix). The model is constrained by the binned density field of Sect. 3 and by the altimetric topography estimate of Sect. 3. The impact of altimetric constraints on the solution uncertainty reduction is compared to that of the dynamical constraints in the three model runs detailed later.

4.1 Run 1. No dynamical constraints except for geostrophy

In run 1, both altimetric data and hydrographic data are used as observational constraints. The density and velocity fields are constrained by the thermal wind relation and the mean dynamic topography by the geostrophic relation. These relations are the only dynamical constraints, mass conservation and tracer conservation are not imposed. This calculation is equivalent to combining via least-squares the mean dynamic topographies computed from altimetry in Sect. 2 and from hydrography in Sect. 3.

The data sets used to compute the two topography estimates span different periods of time, two years for the altimetric data set and 70 y for the hydrographic data set, and it is necessary to define which period is of interest in the present study. Following Ganachaud *et al.* (1997), we consider that the climatological average represented by the hydrographic data base is

the reference. In this case, the uncertainty in the altimetric topography estimate must account for possible inconsistencies between the dynamic topography corresponding to an average over the first two years of T/P data and that corresponding to an average over 70 y. It is not possible to estimate the difference between the two year mean and the climatological mean from the available altimetric data base, but an upper bound on the standard deviation of the dynamic topography due to the interannual variability is given by the mean dynamic topography uncertainty estimate of Fig. 5 which reflects both interannual and seasonal fluctuations. As this upper bound is small compared to the uncertainty in the geoid height model used to compute the altimetric topography, we assume that the difference between the two year mean and the 70 y mean is negligible compared to the geoid height uncertainty. This assumption does not result in inconsistencies in the calculations that follow, and seems to be justified.

The estimated mean dynamic topography is almost identical to the hydrographic estimate of Sect. 3 (Table 1). The associated uncertainty (Fig. 6), however, is reduced compared to that of Sect. 3 (Fig. 5) by about 20% in the Gulf Stream and around $[30^\circ\text{W}, 20^\circ\text{N}]$. This result shows that in the absence of mass and tracer conservation constraints, the altimetric data have a small, but significant, impact on the determination of the mean dynamic topography. This impact, however, is not significant in areas of small uncertainties in the hydrographic estimate of the mean dynamic topography, i.e. in areas of small uncertainties in the density field. It is significant only in regions where error bars in the mean dynamic topography diagnosed from the density field (Fig. 5) are comparable in magnitude to error bars in the mean dynamic topography estimated from altimetric observations (about 20 cm).

4.2 Run 2. All the dynamical constraints

In run 2, we examine whether the altimetric data and the JGM-2 geoid height estimate are consistent with the dynamics of the large-scale ocean circulation. Run 2 is constrained with the same observations as run 1, but the ocean circulation and the associated topography are

Table 1. Column 1: mean uncertainty in the various estimates of the mean dynamic topography ($5^\circ \times 4^\circ$ grid) presented in this paper. Column 2: root mean square of the difference between the $5^\circ \times 4^\circ$ dynamic topography estimate using the dynamical and the altimetric constraints (run 2) and the other $5^\circ \times 4^\circ$ dynamic topography estimates. All the dynamic topography estimates are quite similar

Mean dynamic topography estimate	Mean uncertainty (cm)	Root mean square of topography difference (cm)
T/P-JGM-2	23.1	0.58
Diagnosed from hydrography	10.8	0.39
No dynamical constraints except thermal wind and geostrophy (run 1)	10.5	0.35
All dynamical constraints and altimetry (run 2)	4.8	0
All dynamical constraints but no altimetry (run 3)	4.9	0.03
All dynamical constraints and altimetry, gap in hydrography (run 4)	12.5	0.31
All dynamical constraints but no altimetry, gap in hydrography (run 5)	13.0	0.31

required to satisfy mass, heat, and salt conservation in addition to the thermal wind and geostrophic balances. The Ekman drift derived from the Bunker (1980) wind stress is added to the geostrophic transports in the mixed layer, which is 30 m deep in the model, to represent the direct effect of wind forcing on the circulation.

Mass conservation is imposed within a small error bar (Table 2). Indeed, the density field is adjusted by the inverse model, and the only possible residuals are the mass flux at the air-sea interface and the interior mixing due to the contribution of unresolved small scales (Mercier *et al.*, 1993). These residuals are small compared to the advective fluxes of mass, and mass should be nearly exactly conserved. The potential temperature and salinity fields, on the other hand are not adjusted by the inverse model and they contain a signal due to the eddy variability which is not filtered out. This signal is not consistent with the stationary dynamics of the model, so rather large error bars (Table 2) are required in the corresponding conservation constraints. Similarly, large error bars (Table 2) are associated with the potential vorticity conservation constraint to account for discretization errors and the existence of higher order dynamics near the western boundary.

Several transport constraints are imposed: (1) there is an outflow from the Florida Strait of 30 ± 1 Sv (Niiler and Richardson, 1973); (2) there is no net flux of mass through the northern boundary of the model (the transport across the Bering Strait is 0.8 Sv, Coachman and Aagaard, 1988; for simplicity, the flux across 50°N is taken to be 0 ± 1 Sv in the inverse model calculation). The constraint of no net flux of mass is applied to

all the other zonal sections of the model to enforce the conservation of mass at large scales.

An ocean circulation consistent with the observational constraints and the dynamical constraints is found by the inverse model. After inversion, over 99% of the dynamical constraints are satisfied within one standard deviation, which is better than what one expects from a gaussian distribution. Thus, within the rather large error bar of the JGM-2 geoid height estimate, the mean dynamic topography estimated from T/P altimetric data is consistent with hydrographic data and stationary ocean dynamics. Only marginal consistency was obtained with GEOSAT data despite the very large uncertainties in the GEOSAT altimetric estimate (Martel and Wunsch, 1993). The consistency with T/P data within much reduced error bars compared to those of GEOSAT shows the progress made in the field of altimetry and geodesy in recent years.

The two data sets are consistent even if density errors are neglected, but accounting for these errors is necessary to estimate the uncertainty in the mean dynamic topography. The contribution of the error bars in density to the topography uncertainty is actually four times larger than the contribution of the error bars in reference velocities. Moreover, the uncertainty in the estimated mean dynamic topography hardly changes when uncertainties in the prior estimate of the reference velocities are multiplied or divided by two, but they change significantly if uncertainties in the density field are modified.

The estimated mean dynamic topography (Fig. 7a, b) is similar to the one obtained in the previous section

Table 2. Uncertainty in the dynamical conservation constrain imposed in the inverse model calculations

Constraint	Uncertainty
Source of mass inside a $2.5^\circ \times 2^\circ$ degree box = 0	6×10^5 kg/s (air-sea flux of 1 m/year)
Source of salt inside a $2.5^\circ \times 2^\circ$ degree box = 0	1×10^6 kg/s (imbalance of 1 Sv \times 1%)
Source of heat inside a $2.5^\circ \times 2^\circ$ degree box = 0	4×10^{12} W (imbalance of 1 Sv \times 1°C)
Potential vorticity ($\Delta w - \beta v/f$. $\Delta z = 0$ at the reference level)	1×10^{-5} m/s

UNCERTAINTY IN MEAN DYNAMIC TOPOGRAPHY ESTIMATED BY INVERSE MODEL

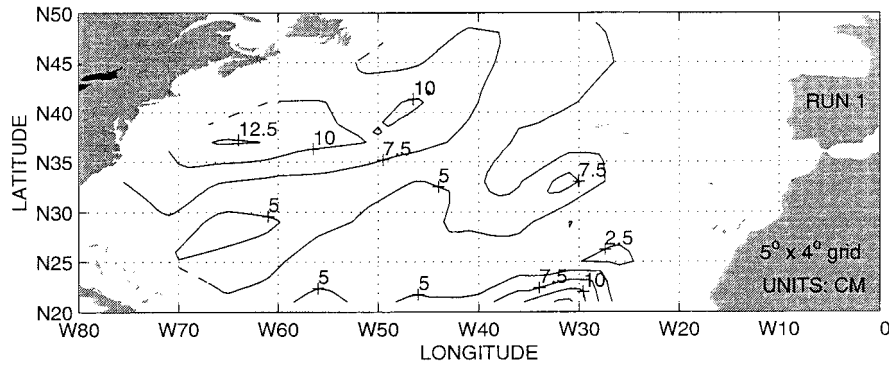


Fig. 6. Uncertainty (cm) in the $5^\circ \times 4^\circ$ mean dynamic topography estimated by the inverse model combining hydrographic and altimetric observations (run 1)

without the conservation constraints (Table 1). The corresponding uncertainty (Fig. 8a, b), however, is much smaller, especially in the Gulf Stream area where the mean dynamic topography is poorly determined from observational constraints alone. Mass conservation and tracer conservation equally contribute to the uncertainty reduction and it is necessary to use all the conservation constraints to obtain the largest uncertainty reduction.

4.3 Run 3. All the dynamical constraints but no altimetry

In run 3, we examine the contribution of the altimetric constraints to the determination of the mean dynamic topography. For that purpose, the inverse model is run

again with all the constraints of run 2 apart from the altimetric constraints. The mean dynamic topography estimated in run 3 and its uncertainty are almost identical to their counterpart in run 2 (Table 1). This result remains valid if the mean dynamic topography estimates are averaged onto a 37.5° longitude by 30° latitude grid, the altimetric constraints reducing the uncertainty in the topography at this large scale by less than 3%. Thus, the altimetric data contribute little to the solution when all the other constraints are used together. This result, consistent with that of Ganachaud *et al.* (1997), indicates that the present geoid height precision is too low for altimetric data to significantly improve our knowledge of the mean circulation at the surface of the North Atlantic.

MEAN DYNAMIC TOPOGRAPHY ESTIMATED BY INVERSE MODEL

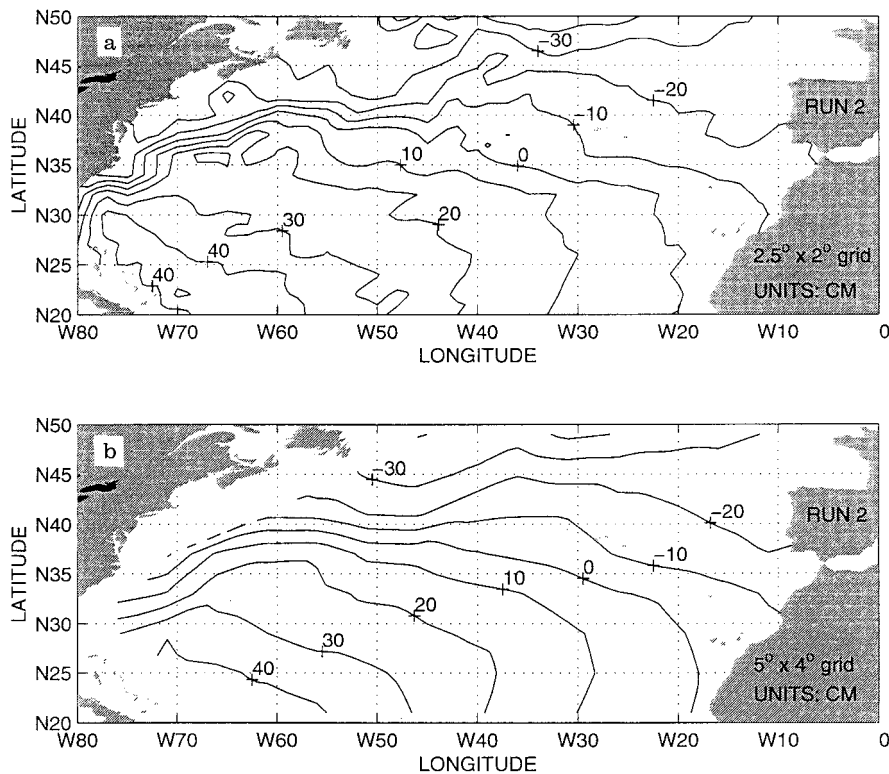


Fig. 7. a Mean dynamic topography (cm) on the $2.5^\circ \times 2^\circ$ grid estimated by the inverse model constrained by dynamical equations, hydrographic observations, and altimetric observations (run 2). **b** Same as **a** but the mean dynamic topography is averaged onto the $5^\circ \times 4^\circ$ grid

UNCERTAINTY IN MEAN DYNAMIC TOPOGRAPHY ESTIMATED BY INVERSE MODEL

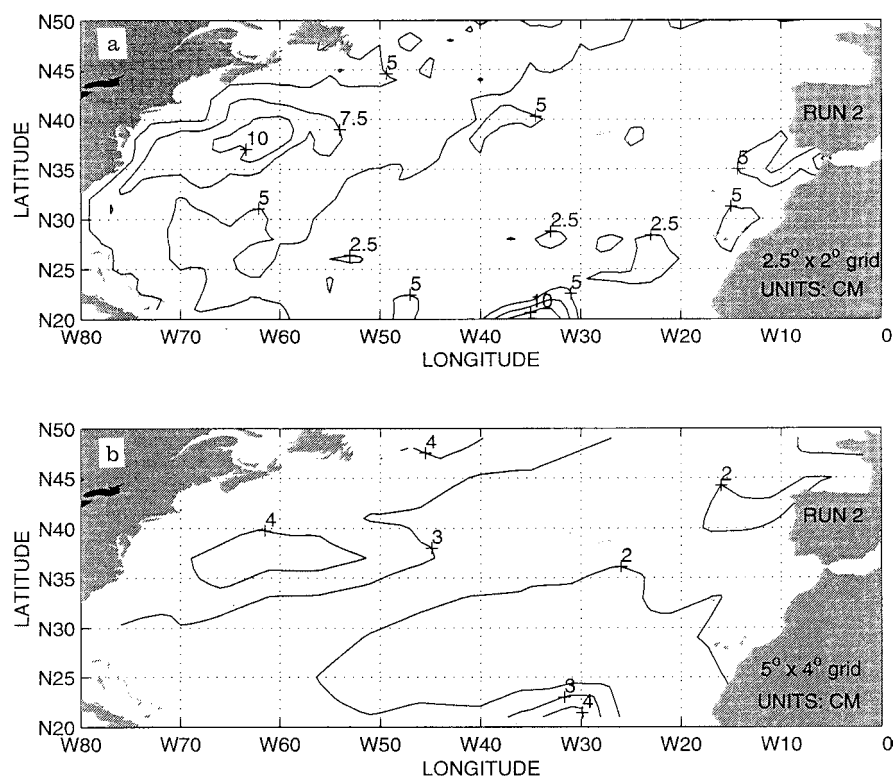


Fig. 8. **a** Uncertainty (cm) in the $2.5^\circ \times 2^\circ$ mean dynamic topography of Fig. 7a. **b** Uncertainty (cm) in the $5^\circ \times 4^\circ$ mean dynamic topography of Fig. 7b

5 Information content of altimetric data in regions where hydrographic data are scarce

It is interesting to examine whether the impact of altimetric constraints could be more significant in regions of the ocean not as well sampled by the hydrographic data base as the North Atlantic. For that purpose, the inverse model is constrained with the density field of the previous sections but with error bars in density multiplied by 10 in a latitude band between 30°N and 40°N . These large error bars simulate the lack of observations of the density field in the large regions between hydrographic sections in calculations using a data base such as that used by Ganachaud *et al.* (1997). They also simulate the situation encountered in poorly sampled ocean basins such as the Southern Ocean. The natural variability of the density field in this basin is difficult to estimate from the sparse hydrographic data base, but we expect it to be of the order of the variability in the Subtropical gyre, i.e. five times the variability in the Subtropical gyre (see the Appendix). Moreover, the density field must be interpolated in the Southern Ocean over large areas void of data, even if a historic data set is used. In view of the large uncertainties introduced in the density field by objective mapping procedures (e.g. Mercier *et al.*, 1993), one can estimate the interpolation errors to double the uncertainties due to the natural variability of the ocean. Thus, the assumption that uncertainties in the density field in poorly sampled and energetic regions like the Southern Ocean are one order

of magnitude larger than in the North Atlantic subtropical gyre is plausible.

Two model runs are performed. One run (run 4) is constrained by the density field with the modified error bars described, all the dynamical constraints, and the altimetric mean dynamic topography estimate of Sect. 2. The other run (run 5) is identical except that the altimetric constraint is not used. In both runs, the resulting mean dynamic topography is similar to that estimated in Sect. 4.2 (Table 1). The uncertainty in both estimates (Fig. 9a,b), however, is much larger than the uncertainty estimated in Sect. 4.2 in the 30°N – 40°N latitude band because of the large uncertainties in the density field in this region.

The altimetric data have a significant impact on those calculations. The uncertainty in the run 4 estimate with altimetric constraint (Fig. 9a) is about 20% smaller than that in the run 5 estimate with no altimetric constraint (Fig. 9b) in the region of the subtropical gyre between 30°N and 40°N . This result shows that altimetric data do have an impact on the determination of the mean dynamic topography when the density field is poorly determined.

This impact can be compared to the impact on reference-level velocity uncertainties calculated by Ganachaud *et al.* (1997). In their calculation, the uncertainties are reduced by less than 1.5% (variance reduced by 3%) almost everywhere when altimetric observations are used, and the maximum uncertainty reduction is 3% (variance reduced by 6%). This reduction is much smaller than the 20% topography uncertainty reduction in the present calculation.

UNCERTAINTY IN MEAN DYNAMIC TOPOGRAPHY ESTIMATED BY INVERSE MODEL

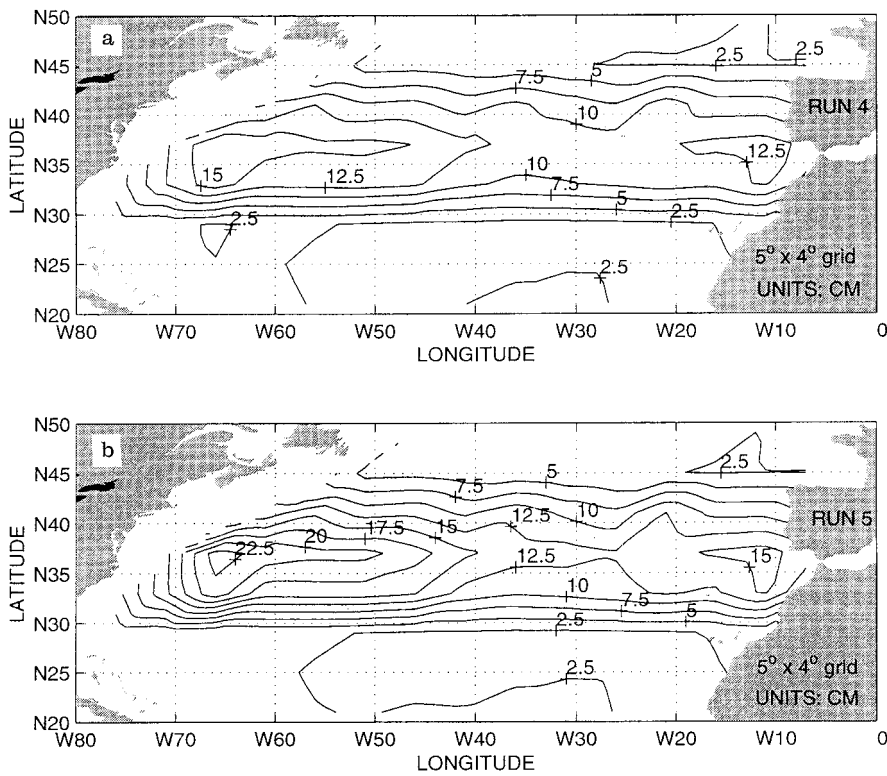


Fig. 9a,b. Uncertainty (cm) in the mean dynamic topography estimated by the inverse model when error bars in the density field are multiplied by 10 in the 30°N–40°N latitude band. **a** With altimetric constraints (run 4); **b** without altimetric constraints (run 5)

Two factors explain the difference between Ganachaud *et al.*'s (1997) conclusion and the present conclusion. First, their calculation can estimate the circulation at the location of oceanic transects only, whereas the present calculation can estimate the circulation in regions where no hydrographic data are available. It is in these regions where the density field is poorly determined that altimetric observations are most likely to provide useful constraints. A second factor is that their study estimates the impact of altimetric observations on the reference level velocities only, whereas the present work estimates the impact on surface quantities like dynamic topography. The impact of altimetric observations on deep reference velocities is smaller than the impact on surface quantities, because the presence of noise in the density field introduces errors, in the integration of the thermal wind relation, that prevent the altimetric information from being transmitted to the deep ocean. This point appears clearly in the present calculation: run 4 shows a 20% reduction of the uncertainty in the mean dynamic topography compared to run 5, but no significant reduction of the uncertainty in the deep reference level velocities. Thus, the difference between the conclusion of the present calculation and that of Ganachaud *et al.* (1997) is explained by the different contexts in which the impact estimates are made and the use of different figures of merit.

In this study, we have deliberately chosen to analyze the results of the various calculations in terms of mean dynamic topography because this quantity is a variable

of the inverse model and its uncertainty can be easily calculated. Moreover, it is a dynamical quantity that is directly linked to geostrophic velocities at the surface of the ocean. This quantity is therefore representative of the circulation in the upper ocean, although it is not clear what depth range it reliably represents. Volume transports can easily be computed from the results of the various inverse calculations but their use to quantify the impact of altimetric observations requires uncertainty estimates. Transport uncertainties are unfortunately difficult to determine because they necessitate the calculation of the full covariance matrix of the density field, and the appropriate software is not available yet for the Mercier *et al.* (1993) model. (The transport uncertainties produced by Paillet and Mercier (1997) neglect correlations in the density field, and are not appropriate for the present study.) All that can be said in the present study is that transports in the upper 100 m of the ocean in run 4 and run 5 differ by a few percent, but it is not possible to tell whether these differences are significant in the absence of transport uncertainty estimates.

Ganachaud *et al.* (1997) estimate the impact of altimetry on oceanic transports but their calculation, based on the impact on the reference velocities, applies to transports over the whole water column and leaves out the impact on transports in the upper ocean that are more likely to be affected by altimetric constraints. Their transport uncertainty calculation neglects the contribution of the uncertainty in relative velocities (Macdonald, 1995), which is likely to dominate in the upper ocean. It

is not clear how their model, which does not treat density as an explicit variable, could account for this contribution.

6 Summary and discussion

The mean dynamic topography calculated by subtracting the JGM-2 geoid height from the T/P mean sea surface height is consistent with a data base of historical hydrographic stations and the dynamics of the large-scale ocean circulation. We find, in accordance with Ganachaud *et al.*'s (1997) results, that this topography estimate only weakly constraints an inverse estimate of the mean ocean circulation in the North Atlantic. However, altimetric observations significantly constrain the surface circulation when uncertainties in the density field are increased to represent regions of the ocean where the hydrography is poorly determined. This result moderates the conclusion of no significant impact of the altimetric data drawn by Ganachaud *et al.* (1997) from a calculation at the location of hydrographic sections and based on deep reference level velocities only.

Depending on the area considered, the uncertainty in the inverse modeling estimate of the mean dynamic topography (Fig. 8b) is between five and ten times smaller than that in the altimetric estimate using the JGM-2 geoid (about 20 cm). Therefore, by subtracting the inverse topography estimate from the T/P mean sea surface height one can expect to obtain a geoid height estimate that is significantly improved compared to existing models. As an illustration of this point, a

correction to the JGM-2 geoid height is estimated from the results of the inverse calculation of Sect. 4.2 (run 2). This correction is on the order of 10 cm for the geoid height estimated on the 5° longitude by 4° latitude grid (Fig. 10a). It is larger near continental margins which makes physical sense (Fig. 10a). The difference between the inverse and the JGM-2 geoid height estimates decreases with increasing scales (Fig. 11) and is within the JGM-2 height uncertainty (Nerem *et al.*, 1994, see their Fig. 6). At small scales, the difference between the recent EGM-96 (Lemoine *et al.*, 1997) height estimates and the corrected estimate is slightly smaller than the difference between the JGM-2 estimate and the corrected estimate (Fig. 11). This result is encouraging because departures from the JGM-2 estimate are penalized in the inverse calculation whereas no information is given to the model about the EGM-96 estimate. It is consistent with the idea of the corrected estimate being the best available estimate of the geoid height at small scales, followed by the EGM-96 estimate, the JGM-2 estimate being the least accurate. At spatial scales larger than about 5° degrees, the inverse estimate is less consistent with the EGM-96 estimate than with the JGM-2 estimate which suggests that the correction is an improvement at small scales only. However, because the EGM-96 and the JGM-2 geoid height estimates are both quite uncertain, their use to test the corrected estimate is not conclusive and it is necessary to calculate the uncertainty in the corrected geoid height.

This uncertainty (Fig. 10b) depends on the uncertainty in the mean dynamic topography calculated by the inverse procedure which takes into account model-

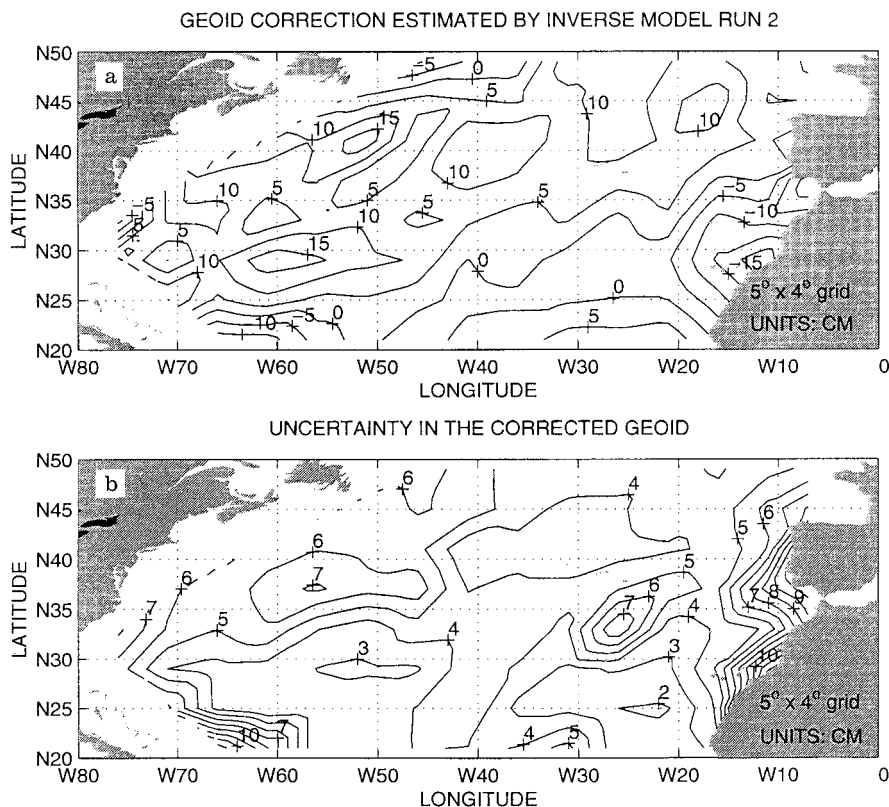


Fig. 10. **a** Correction to the geoid height (cm) estimated on the $5^\circ \times 4^\circ$ grid by the inverse model (run 2). **b** Uncertainty (cm) in the $5^\circ \times 4^\circ$ corrected geoid height estimate

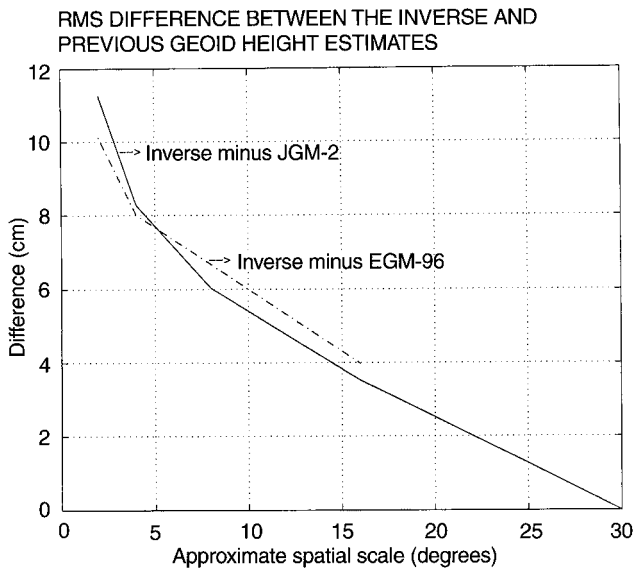


Fig. 11. Root mean square difference as a function of scale between the inverse model geoid height estimate and: the JGM-2 estimate (solid line); the EGM-96 estimate (dot-dashed line)

ling errors and observational errors. Modelling errors (Table 2) have been difficult to estimate, but their precise determination is not critical. The difference between the topography uncertainty in a variant of run 2 with modelling errors multiplied by two and the uncertainty in a variant of run 2 with modelling errors divided by two is on the order of 1 cm in the Gulf Stream, and less than 1 cm elsewhere. Observational errors are estimated directly from the data, and they are plausible despite the crude approximations made in their calculation. The uncertainty in the density field is carefully estimated in the present calculation (Appendix). The uncertainty in the T/P sea surface height is calculated directly from altimetric observations and, for the sake of simplicity, is assumed to be decorrelated from that of the mean dynamic topography estimated by the inverse model (the assumption of no correlation would be rigorous if the topography estimated in run 3 were used instead of that estimated in run 2). All the sources of uncertainty in the geoid height estimate have thus been accounted for in this calculation, and the result should be reliable.

The total geoid height uncertainty is on the order of 5 cm in the interior of the ocean at the scale of the $5^\circ \times 4^\circ$ grid, and is about one third of the corresponding uncertainty in the JGM-2 estimate. The uncertainties are higher near the continents because the sea surface height is not precisely known there, the number of independent altimetric observations being small in the boxes that intersect the continents.

The 5 cm precision is as good as that expected from intermediate gravimetry missions (Minster, personal communication, 1996). Only the GOCE mission would provide a higher precision, of the order of the centimeter (Minster, personal communication, 1996), but it will take several years before such a mission can be launched. The main difficulty to overcome in order to

estimate the geoid height over the global ocean using an inverse model of the ocean circulation is to determine the mean density field and its uncertainty. The hydrographic data base is scarce outside of the North Atlantic, and a global geoid height estimate will not be as precise as the North Atlantic estimate. In these regions where the density field is poorly known, however, altimetric constraints will yield a significant improvement of mean circulation estimates in the upper ocean, and an inverse modelling combination of these constraints with hydrographic and dynamical constraints will still be useful.

Acknowledgements. The inverse calculations presented in this work were carried out on the IFREMER CONVEX computer. We are grateful to R. Rapp for providing the spatial autocorrelation function of the JGM-2 geoid and to P.-Y. Le Traon for providing the mean dynamic topography calculated using the T/P observations and the JGM-2 geoid. Discussions with G. Larnicol and J.-F. Minster helped us with the interpretation of the inverse calculations. We thank C. Wunsch and two anonymous reviewers for their useful comments on the draft version of this paper. Tim Boyer made the National Oceanographic Data Center hydrographic data available to us and we acknowledge his assistance in compiling the data base used in this study. C. Maillard and M. Fichaut also helped with the preparation of the hydrographic data base. This work was supported in part by the French Programme National d'Etude de la Dynamique du Climat.

Topical Editor D. J. Webb thanks V. Zlotnicki and P. Challenor for their help in evaluating this paper.

Appendix: processing of the hydrographic data base

The hydrographic stations compiled for this study are too numerous (over 100 000 stations) to be directly used in the inverse calculation. The hydrographic data are therefore processed to produce a climatology of the mean density field over the model finite difference grid (Fig. 1). The various steps of this data reduction are similar to those used in Reynaud (1996) in the context of an atlas of the entire Atlantic and are summarized here.

The first step in the data processing consists in projecting the salinity and temperature profiles associated with each hydrographic station onto the 35 vertical levels of the inverse model (Mercier *et al.*, 1993). In practice, high resolution CTD stations are decimated, whereas low resolution bottle stations are interpolated using a cubic spline interpolator. The procedure is designed so that shallow stations are not extrapolated to deep levels of the ocean. Stations that do not satisfy the following quality requirements are rejected: salinity and temperature values inside a reasonable range, no local potential density inversion, no anomalous salinity or temperature peaks (Reynaud, 1996). These quality checks validate about 75% of the stations. Density is then calculated from the validated salinity and temperature fields at each standard level.

The second step consists in gridding the density profiles by averaging them inside 2.5° longitude \times 2° latitude boxes centred on the inverse model density grid (Fig. 1). This procedure, which is simpler than the averaging inside radii of influence done by Reynaud

(1996), is possible here because the boxes are quite large and the data coverage in the North Atlantic is such that several stations are available in most boxes. The mean density and its standard deviation are computed in boxes that contain at least four validated stations. As a final validation test, density values that are further than three standard deviations away from the mean are discarded, and the mean is recomputed. The values corresponding to the few 2.5° longitude \times 2° latitude boxes that contain less than four validated data points are flagged. At this stage, we have a set of climatological density values on the inverse model grid that we call the $\langle\langle$ binned density field $\rangle\rangle$.

The third step to reduce the volume of data used in the inverse model is a vertical empirical orthogonal function (EOF) decomposition of the binned density field. In practice, 10 modes are sufficient to represent over 90% of the variance in this field, and the EOF decomposition reduces the number of variables by a factor of three. The density field at 700 m depth is reconstructed (Fig. 12a) using the first ten EOFs. Despite the coarse resolution, the reconstructed density field exhibits a Gulf Stream front that is much sharper than that of the Levitus *et al.* (1994) atlas.

Carefully estimating the uncertainty in the density field, and thus the uncertainty in the EOF coefficients, is critical for the accuracy of the inverse calculations. Several approaches are available for that purpose, and it is not obvious which one is best. The objective mapping approach used by Mercier *et al.* (1993) and Le Traon and Mercier (1992) has the advantage of being easy to implement, but it shows a tendency to underestimate the

uncertainty. This point is evidenced by the small uncertainties in surface velocities diagnosed from the objectively mapped EOF coefficients. These uncertainties are on the order of a few cm/s in the Gulf Stream area² (Mercier *et al.*, 1993), which is unrealistically small for an unstable jet like the Gulf Stream. (In Mercier *et al.* (1993), uncertainties in the density field, and uncertainties in velocities diagnosed from the density field, are high in the northeastern Atlantic. These high uncertainties correspond to regions that are poorly covered by the hydrographic data base used in their study, and they are solely due to interpolation errors.) The underestimation of the uncertainties in the EOF coefficients is due to the smoothing of the data introduced by the objective mapping procedure that tends to filter out most of the mesoscale variability. This underestimation is most obvious near sharp density fronts such as the Gulf Stream because the effect of smoothing is large there.

A different approach is used in the present work to estimate the uncertainty in the EOF coefficients, associated with the binned density field at each grid point of the model. Inside each $2.5^\circ \times 2^\circ$ box defined by the model grid, all the vertical profiles of density corresponding to validated stations are projected onto the eigen vectors of the EOF decomposition of the binned density field. This projection produces a local estimate of the EOF coefficients at each station. It is then straightforward to compute the standard deviation of these local coefficients inside the $2.5^\circ \times 2^\circ$ boxes to estimate the uncertainty in the binned coefficients. The magnitude of the uncertainty in the binned EOF coefficients depends on the size of the bin used in the

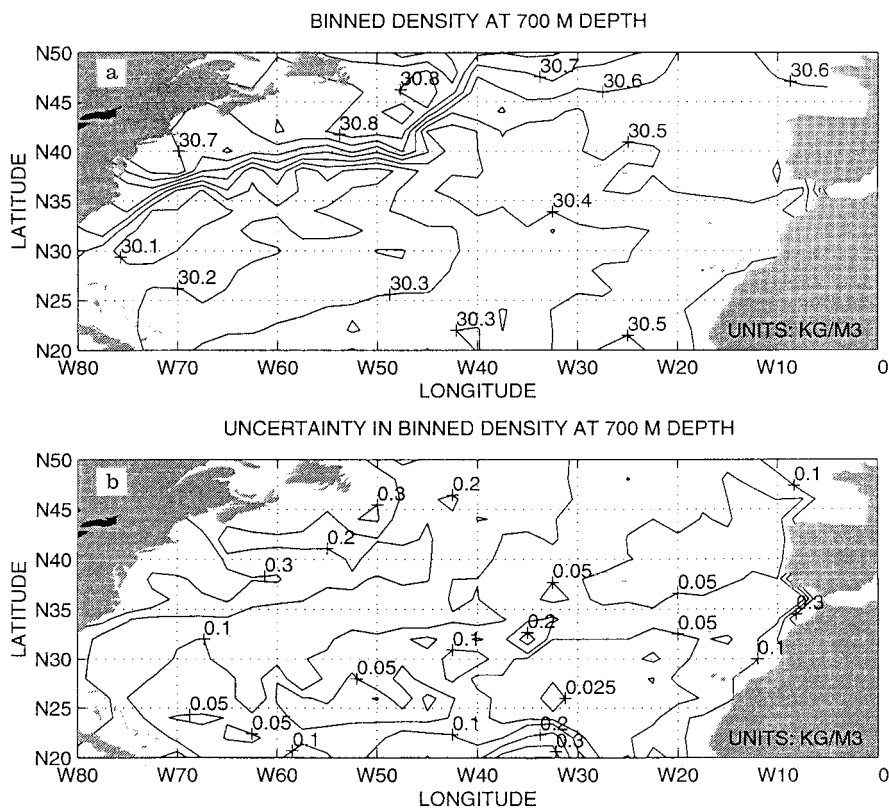


Fig. 12. **a** Density field ($\text{kg}\cdot\text{m}^{-3}$) binned onto the 2.5° longitude \times 2° latitude grid at 700 m depth. **b** Uncertainty ($\text{kg}\cdot\text{m}^{-3}$) in the binned density field at 700 m depth

present gridding procedure because of spatial inhomogeneities in the density field caused by fronts such as the Gulf Stream. Therefore, this bin size must be consistent with the resolution of the inverse model in order to properly estimate the uncertainty in the density field used in the model.

The calculation of the EOF coefficients full covariance matrix is feasible in principle, but it is not attempted here because of the computational load required for the treatment of more than 100 000 hydrographic stations. Thus we assume that there is no correlation between the EOF coefficients of distinct bins. The plausibility of the map of uncertainty in the density-diagnosed mean dynamic topography (Fig. 5) indicates that this assumption does not result in major inconsistencies with what is known of the circulation in the North Atlantic. Moreover, the density field is used to constrain the inverse model, and the model introduces large-scale correlations into this field through the mass and tracer conservation equations.

As a final step, the binned EOF coefficients and the associated uncertainties are interpolated over the few $2.5^\circ \times 2^\circ$ boxes that do not contain enough validated data points to compute meaningful estimates of the mean and of the standard deviation (a minimum of four data points is required). The interpolated uncertainty is then subjectively multiplied by two to account for interpolation errors.

The uncertainty in the density field at 700 m depth reconstructed from the first ten EOFs (Fig. 12b) is much larger than that obtained by Mercier *et al.* (1993). It is about five times larger in the Western Atlantic than in the Eastern Atlantic, which is consistent with the idea that the mesoscale activity is more intense near sharp fronts like the Gulf Stream. This realistic uncertainty yields the plausible estimates of the uncertainty in the mean dynamic topography presented here.

References

- Bunker, A. F.**, Trends of variables and energy fluxes over the Atlantic Ocean from 1948 to 1972, *Mon. Weather Rev.*, **108**, 720–732, 1980.
- Coachman, L. K., and K. Aagaard**, Transport through the Bering Strait: annual and interannual variability, *J. Geophys. Res.*, **93**, 15 535–15 539, 1988.
- Ganachaud, A., C. Wunsch, M.-C. Kim, and B. Tapley**, Combination of TOPEX/POSEIDON data with a hydrographic inversion for determination of the oceanic general circulation and its relation to geoid accuracy, *Geophys. J. Int.*, **128**, 708–722, 1997.
- Lemoine *et al.***, 1997, web site: <http://cdadis.gsfc.nasa.gov/926/egm96/egm96.html>.
- Levitus, S., R. Burgett, and T. P. Boyer**, *World Ocean Atlas NESDIS*, vol. 3: salinity, and vol 4: temperature, National Oceanographic Data Center, 1994.
- Le Traon, P.-Y., and H. Mercier**, Estimating the North Atlantic mean surface topography by inversion of hydrographic and lagrangian data, *Oceanol. Acta*, **15**, 563–566, 1992.
- Macdonald, A.**, Oceanic fluxes of mass, heat and freshwater: a global estimate and perspective, Ph.D. Thesis, Department of Earth, Atmospheric, and Planetary Sciences, Massachusetts Institute of Technology, Cambridge, MA, 1995.
- Martel, F., and C. Wunsch**, Combined inversion of hydrography, current meter data and altimetric elevations for the North Atlantic circulation, *Manuscr. Geod.*, **18**, 219–226, 1993.
- Mercier, H., M. Ollitrault, and P.-Y. Le Traon**, An inverse model of the North Atlantic general circulation using Lagrangian float data, *J. Phys. Oceanogr.*, **23**, 689–715, 1993.
- Nerem, R. S., F. J. Lerch, J. A. Marshall, E. C. Pavlis, B. H. Putney, B. D. Tapley, R. J. Eanes, J. C. Ries, B. E. Schutz, C. K. Shum, M. M. Watkins, S. M. Klosko, J. C. Chan, S. B. Luthcke, G. B. Patel, N. K. Pavlis, R. G. Williamson, R. H. Rapp, R. Biancale, and F. Nouel**, Gravity model development for TOPEX/POSEIDON: joint gravity models 1 and 2, *J. Geophys. Res.*, **99**, 24 421–24 447, 1994.
- Niiler, P. P., and W. S. Richardson**, Seasonal variability of the Florida Current, *J. Mar. Res.*, **31**, 144–167, 1973.
- Paillet, J., and H. Mercier**, An inverse model of the eastern North Atlantic general circulation and thermocline ventilation, *Deep-Sea Res. I*, **44**, 1293–1328, 1997.
- Reynaud, T.**, Modélisation inverse de l'Atlantique - Partie 1: Traitement des données hydrographiques, *Technical Report of the Laboratoire de Physique des Océans*, Brest, 1996.
- Roemmich, D., and C. Wunsch**, On combining satellite altimetry with hydrographic data, *J. Mar. Res.*, **40**, 605–619, 1982.
- Tapley, B. D., J. C. Ries, G. W. Davis, R. J. Eanes, B. E. Schutz, C. K. Shum, M. M. Watkins, J. A. Marshall, R. S. Nerem, B. H. Putney, S. M. Klosko, S. B. Luthcke, D. Pavlis, R. G. Williamson, and N. P. Zelensky**, Precision orbit determination for TOPEX/POSEIDON, *J. Geophys. Res.*, **99**, 24 383–24 404, 1994.
- White, B. W., and C.-K. Tai**, Inferring interannual changes in global upper ocean heat storage from TOPEX altimetry, *J. Geophys. Res.*, **100**, 24 943–24 954, 1995.